

1 **The effects of meteorological parameters and**
2 **diffusive barrier reuse on the sampling rate of**
3 **a passive air sampler for gaseous mercury**

4
5 David S. McLagan,¹ Carl P. J. Mitchell,¹ Haiyong Huang,¹ Batual Abdul Hussain,¹ Ying Duan Lei,¹
6 Frank Wania^{1,*}

7
8 ¹ Department of Physical and Environmental Sciences, University of Toronto Scarborough, 1065
9 Military Trail, M1C 1A4, Toronto, Ontario, Canada

10

11 * Corresponding Author – email: frank.wania@utoronto.ca; phone: +1 416-287-7225

12 **ABSTRACT**

13 Passive air sampling of gaseous mercury (Hg) requires a high level of accuracy to discriminate
14 small differences in atmospheric concentrations. Meteorological parameters have the potential
15 to decrease this accuracy by impacting the sampling rate (*SR*), i.e., the volume of air that is
16 effectively stripped of gaseous mercury per unit of time. We measured the *SR* of a recently
17 calibrated passive air sampler for gaseous Hg in the laboratory under varying wind speeds
18 (wind-still to 6 m s⁻¹), temperatures (-15 to +35 °C), and relative humidities (44 to 80 %). While
19 relative humidity has no impact on *SR*, *SR* increases slightly with both wind speed (0.003 m³
20 day⁻¹ increase in *SR* or 2.5 % of the previously calibrated *SR* for every m s⁻¹ increase for wind
21 speeds > 1 m s⁻¹, typical of outdoor deployments) and temperature (0.001 m³ day⁻¹ increase in
22 *SR* or 0.7 % for every 1 °C increase). The temperature dependence can be fully explained by the
23 effect of temperature on the molecular diffusivity of gaseous mercury in air. Although these
24 effects are relatively small, accuracy can be improved by adjusting *SR*s using measured or
25 estimated temperature and wind speed data at or near sampling sites. We also assessed the
26 possibility of reusing Radiello® diffusive barriers previously used in the passive air samplers. The
27 mean rate of gaseous Hg uptake was not significantly different between new and previously
28 used diffusive barriers in both lab and outdoor deployments, irrespective of the applied
29 cleaning procedure. No memory effect from Radiellos® previously deployed in a high Hg
30 atmosphere was observed. However, a loss in replicate precision for the dirtiest Radiellos® in
31 the indoor experiment suggests that cleaning is advisable prior to reuse.

32 **KEYWORDS**

33 Passive air sampling, Hg, atmosphere, calibration, green chemistry

34 1. INTRODUCTION

35 Fine spatial resolution measurements of atmospheric contaminants are difficult and expensive,
36 especially at remote locations and in developing countries. By allowing for simultaneous, cost-
37 effective measurements at a multitude of sites, passive air samplers (PASs) are useful,
38 complementary monitoring tools in atmospheric science. PASs can be deployed in high
39 numbers, at sites away from sources of electricity, and in locations where the costs and logistics
40 of active sampler deployments can be prohibitive (McLagan et al., 2016a). In order for a PAS to
41 yield volumetric air concentration data, a sampling rate (*SR*), i.e., the volume of air that is
42 effectively stripped of the contaminant of concern per unit of time, needs to be derived. This is
43 done either in calibration experiments that deploy the PAS concurrently with reliable active
44 sampling techniques or theoretically based on an understanding of the processes controlling
45 mass transfer from atmosphere to PAS sorbent (Armitage et al., 2013; Gustin et al., 2011; Skov
46 et al., 2007). Any uncertainty and bias in the *SR* is directly propagated to the volumetric air
47 concentration derived from a PAS. Accordingly, a reliable PAS requires that the impact of
48 various factors influencing the *SR* is, in order of preference, either eliminated, minimized or
49 quantifiable and predictable.

50 A common conceptual model of uptake in PASs assumes a stagnant air layer or air-side
51 boundary layer (ASBL) around the sorbent, through which contaminant transfer occurs solely by
52 molecular diffusion (McLagan et al., 2016a; Shoeib and Harner, 2002). Wind decreases the
53 thickness of the ASBL which in turn increases the *SR* (Bartkow et al., 2005; Moeckel et al., 2009;
54 Pennequin-Cardinal et al., 2005). Diffusive barriers aim to reduce the influence of wind by
55 standardizing the molecular diffusion distance to the sorbent and thereby ensuring that the
56 diffusive component of contaminant transfer is the rate limiting step (Huang et al., 2014;
57 Lozano et al., 2009; McLagan et al., 2016a). For PASs with diffusive barriers the ASBL is shifted
58 from the outside of the sorbent to the outside of the diffusive barrier (McLagan et al., 2016b).
59 While a diffusive barrier thus reduces the relative contribution of the ASBL to the overall
60 diffusion distance, it cannot entirely mitigate *SR* variability caused by wind (Pennequin-Cardinal
61 et al., 2005; Plaisance et al., 2002; Skov et al., 2007). Protective shields around the sorbent or

62 diffusive barrier are often employed to further reduce the influence of wind by reducing the
63 face velocities at these surfaces. However, like diffusive barriers, they too are not likely to
64 completely eliminate the influence of wind on the thickness of the ASBL (Huang et al., 2014).

65 Temperature has the potential to affect *SR* in two ways: (i) changing the rate of gas phase
66 diffusion of the contaminant due to the temperature dependence of molecular diffusion
67 coefficients (Armitage et al., 2013; Huang et al., 2014; Lozano et al., 2009); and (ii) shifting the
68 partitioning equilibria between the sorbent and the gas phase (Armitage et al., 2013; Lozano et
69 al., 2009; McLagan et al., 2016a). Relative humidity (RH) may affect *SRs* by influencing the
70 sorptive properties of certain sorbents for target analytes (Huang et al., 2014). Other factors
71 that may affect the sorption of contaminants to PAS sorbents include passivation of sorbents
72 (interfering compounds blocking sorbent uptake sites or stripping analytes through reaction)
73 (Brown et al., 2012; Gustin et al., 2011), degradation of the sorbent over time (Brown et al.,
74 2011; McLagan et al., 2016a), and uptake of the contaminant to the sampler housing or
75 diffusive barrier (Gustin et al., 2011; Huang et al., 2014; McLagan et al., 2016a).

76 Mercury is a persistent, bioaccumulative, and toxic contaminant of global concern that has
77 come under greater international scrutiny with the adoption of the Minamata Convention
78 (UNEP, 2013). A key stipulation under Article 19 of the convention “Research, Development and
79 Monitoring” is the requirement of participating parties to improve current monitoring networks
80 (UNEP, 2013). A PAS for measuring atmospheric Hg could play an important role in this context,
81 if it can be shown to be suitable for monitoring long-term background concentrations,
82 concentration gradients in and around Hg sources, and personal exposure levels (McLagan et
83 al., 2016a). Gaseous elemental Hg (GEM) is generally the dominant form of atmospheric Hg
84 (typically making up >95 %), due to its high atmospheric residence time of ~1 year (Driscoll et
85 al., 2013; Pirrone et al., 2010; Selin, 2009), especially at sites remote from combustion sources
86 (McLagan et al., 2016a; Peterson et al., 2009; Rutter et al., 2009). The long atmospheric
87 residence time of GEM results in fairly uniform background concentrations within each
88 hemisphere, with much of the global atmosphere having levels within <25 % of the hemispheric
89 average (Gustin et al., 2011). PASs capable of discriminating such small concentration variability

90 require high accuracy and precision, i.e. *SRs* need to be well characterized and repeatable.
91 Existing PASs for gaseous mercury have struggled to achieve the accuracy and precision
92 necessary for background monitoring due to inadequate detection limits or highly variable *SRs*
93 (Huang et al., 2014; McLagan et al., 2016a).

94 We recently introduced a PAS for gaseous Hg with a precision based uncertainty of $2 \pm 1 \%$ that
95 uses an activated carbon sorbent and a Radiello® diffusive barrier (McLagan et al., 2016b).
96 While it is believed that the sampler takes up predominantly GEM, we cannot rule out the
97 possibility for gaseous oxidized Hg to also pass through the diffusive barrier (McLagan et al.,
98 2016b). We therefore use the term gaseous Hg to define the target analyte. An earlier
99 calibration of this PAS at one outdoor location yielded a *SR* of $0.121 \text{ m}^3 \text{ day}^{-1}$ (McLagan et al.,
100 2016b). Here we report on a series of laboratory experiments that quantified the effect of wind
101 speed, temperature, and RH on the *SR* of that sampler. We additionally explored the possibility
102 of reusing the Radiello® diffusive barrier in multiple deployments in order to further reduce the
103 costs associated with the sampler's use. During deployment, the inside of the Radiello® can
104 become covered in sorbent dust. It is also possible that atmospheric components, e.g.
105 atmospheric particulate matter and oxidants, sorb to or react with the diffusive barrier during
106 deployment. Thus, in addition to meteorological impacts on the PAS's *SR*, we also explored the
107 effect of prior use and cleaning of the diffusive barrier on the uptake of Hg in the PAS.

108 **2. METHODS**

109 **2.1 Sampler Design**

110 The sampler consists of a porous stainless steel mesh cylinder, filled with ~0.7 g of sulphur-
111 impregnated activated carbon sorbent (HGR-AC; Calgon Carbon Corp.), which is inserted into a
112 Radiello® radial diffusive body (Sigma Aldrich), which itself is placed inside a polyethylene-
113 terephthalate protective jar. During deployments the opening of the jar, covered with a
114 polypropylene (PP) mesh screen, is facing down. After sampling the jar is sealed tightly with a
115 PP cap, PTFE tape wrapped around seal, and placed in double resealable plastic bags for
116 transport and storage. McLagan et al. (2016b) provide more detail on the PAS design.

117 2.2 Study Design

118 2.2.1 *WIND*. PAS in four different configurations were exposed to different wind conditions in
119 the laboratory at the University of Toronto Scarborough: (1) regular, white Radiello® with
120 windshield, (2) white Radiello® without windshield, (3) thick-walled, less porous, yellow
121 Radiello® with windshield, and (4) yellow Radiello® without windshield. Adopting the
122 experimental setup of Zhang et al. (2013), electronic fans (Delta Electronics Inc., model number:
123 BFC1212B) were employed to generate wind for each individual sampler. The angle of wind
124 incidence was always 90°, i.e. we simulated wind that is blowing parallel to the surface. Wind
125 speeds of 1, 1.5, 2, 3, 4, 5, and 6 m s⁻¹ were achieved by manipulating the distance between
126 PASs and fan (see Fig. S1 and Fig. S2). For each wind speed triplicate PASs were deployed. Wind
127 speeds for each individual PAS were measured every 5 seconds with a hot-wire
128 Anemometer/Thermometer (Traceable®, VWR International) for five minutes before and five
129 minutes after each deployment. As such, average wind speeds of individual samplers within
130 each wind speed treatment varied slightly (Fig. 1). “Wind-still” experiments without fans were
131 performed for comparison (with wind speed assumed to be 0.05 m s⁻¹).

132 While experiments with white Radiellos (configuration 1 and 2) generally lasted one week,
133 additional experiments lasting two, three, and four weeks were performed at selected wind
134 speeds (3 and 6 m s⁻¹). Experiments with yellow Radiellos (configurations 3 and 4) lasted two
135 weeks (the lower *SR* of yellow Radiello® requires longer deployment times to reach detection
136 limits) and were only performed at wind speeds of 3 and 6 m s⁻¹, as well as without fans.
137 Additionally, a 3 months uptake experiment under wind-still conditions was performed in order
138 to obtain a precise *SR* of the PAS with a white Radiello deployed indoors with a protective
139 shield. Eighteen samplers were deployed at the same time and triplicates were removed after
140 15, 28, 46, 56, 70 and 84 days. The earlier indoor calibration experiment described in McLagan
141 et al. (2016b) had been performed without a windshield.

142 Temperature and RH, monitored before, after, and periodically during each individual
143 experiment, ranged from +21.9 to +24.2 °C and from 32 – 53 %. While there was some variation

144 in the gaseous Hg concentration as recorded by the Tekran 2537A between deployments, the
 145 average concentration across all wind experiments was $1.9 \pm 0.3 \text{ ng m}^{-3}$.

146 **2.2.2 TEMPERATURE & RELATIVE HUMIDITY.** The regular PAS configuration (configuration 1)
 147 was exposed to eight different combinations of temperature and RH (Table 1) for two weeks
 148 periods in climate controlled walk-in chambers located at the Biotron Facility of Western
 149 University in London, Ontario. Each treatment included five replicates, all deployed in the same
 150 chamber over the same time period. Samplers were attached to metal shelving units near the
 151 centre of the chambers where a continuous flow of air from the outflow of the climate control
 152 units of $1.1 - 2.3 \text{ m s}^{-1}$ was observed using the hot-wire Anemometer over a two minute period
 153 at the completion of each experiment. The average actively measured gaseous Hg
 154 concentration across all temperature and RH experiments was $2.2 \pm 0.9 \text{ ng m}^{-3}$.

155 **Table 1: Table 1: Combinations of temperature and relative humidity during the eight experiments**
 156 **performed in climate-controlled chambers. The three relative humidity treatments were 44, 60, and**
 157 **80 % while the temperature was held constant at 20 °C. All treatments were used for the temperature**
 158 **experiments**

| | | | | | | | | |
|-----------|-----------|---------|----------|----------|----------|----------|----------|----------|
| Temp (°C) | -15.0±0.1 | 5.0±0.0 | 12.5±0.1 | 19.9±0.0 | 20.0±0.1 | 20.0±0.1 | 27.5±0.0 | 35.0±0.0 |
| RH (%) | 68±1 | 77±1 | 76±2 | 44±5 | 60±1 | 80±0 | 60±1 | 45±3 |

159 **2.2.3 RADIELLO® REUSE.** The potential impacts of sorbent dust accumulation or atmospheric
 160 contamination during prolonged deployment periods on sampling rates and therefore on the
 161 ability to reuse the Radiello® diffusive barriers are unknown. Currently, new diffusive barriers
 162 are used for each deployment. In this experiment, previously used Radiellos® were redeployed
 163 after different cleaning procedures were applied. Six cleaning treatments were applied: *new*
 164 (unused Radiellos®), *uncleaned* (unaltered after previous deployments), *physical* (physical
 165 agitation with funnel brushes and compressed air blow down), *soap* (Citranox® detergent,
 166 cleaning brushes, and deionized water, compressed air blow down, deionized water rinse and
 167 sonication and air drying), *acid* (six hour soak in 20 % HNO₃ bath, deionized water rinse,
 168 compressed air blow down, deionized water rinse and sonication and air drying), and *heat-acid*
 169 (six hour soak in 20 % HNO₃ bath at 40 °C, deionized water rinse, compressed air blow down,

170 deionized water rinse and sonication and air drying). All Radiellos® in each cleaning treatment
171 were cleaned once according to the aforementioned methods. Prior to cleaning, diffusive
172 bodies were categorized based on the extent of visible dust coating using a 5-point scale (0 –
173 new, 1 – very low, 2 – low, 3 – moderate, 4 – high, and 5 – very high; see Fig. S3). To the extent
174 this was possible with a limited stock of previously deployed Radiellos®, we evenly distributed
175 Radiellos® of variable dust coating among the treatments (see Table S2 for details). We also
176 tested Radiellos® previously deployed in contaminated environments with very high gaseous Hg
177 concentrations ($\sim 100 - 10000 \text{ ng m}^{-3}$) to assess whether such deployments led to a memory
178 effect whereby sorbed Hg is released from the diffusive body during subsequent uses. All
179 samplers from this *memory* treatment contained moderate dust coating and were not cleaned.

180 Five replicate samplers for each of the 7 treatments were deployed for a period of two weeks in
181 a laboratory with slightly elevated Hg concentrations (previously measured as $\sim 5-10 \text{ ng m}^{-3}$) at
182 the University of Toronto Scarborough. Additionally, five different replicate samplers for each
183 of the three treatments *new*, *uncleaned*, and *soap* were exposed for 34 days outdoors on the
184 campus of the University of Toronto Scarborough (43.78714 °N, 79.19049 °W). In this case, all
185 previously used Radiellos® were heavily dust coated (category 4 or 5, see Table S3 for details).
186 In both the indoor and outdoor experiment all samplers were deployed concurrently.
187 Therefore, no active gaseous Hg measurements were necessary and the mass of sorbed Hg
188 could be directly compared and was used in data analysis.

189 **2.2.4 ACTIVE GASEOUS MERCURY MEASUREMENTS.** A Tekran 2537A (Tekran Instruments Corp.)
190 was used to measure the gaseous Hg concentrations at 5 min intervals throughout all wind,
191 temperature and RH experiments. A sampling inlet that combined a 2 m Teflon tube connected
192 to a 0.2 μm PTFE filter was used (detailed setup is given in: (Cole and Steffen, 2010; Steffen et
193 al., 2008)). Auto-calibrations were made using the internal Hg permeation unit every 25 hrs and
194 these were verified through manual injections from a Tekran 2505 Mercury Vapor Primary
195 Calibration Unit (Tekran Instruments Corp.) before and after each set of experiments. Quality
196 control and assurance of the Tekran 2537A data sets followed the Environment Canada
197 Research Data Management and Quality Control system (Steffen et al., 2012).

198 2.2.5 SAMPLING RATE CALCULATION. SRs ($m^3 \text{ day}^{-1}$) were calculated using:

$$199 \quad SR = m / (C t) \quad (1)$$

200 where m is the mass of sorbed mercury (ng), C is the concentration of gaseous Hg measured by
201 the Tekran 2537A ($ng \text{ m}^{-3}$), and t is the deployment time of the PAS (days). With the exception
202 of the 3-months experiment, the SRs were derived from the sorbed Hg (m) in individual PAS
203 deployments using Eq. (1). SRs derived from a single deployment generally have a higher
204 uncertainty than SRs derived from experiments involving multiple simultaneous deployments of
205 variable length, such as those described in McLagan et al. (2016b). This uncertainty is further
206 increased when deployment times are short and gaseous Hg concentrations are low, as m will
207 be closer to quantification limits. Nevertheless, to constrain the uncertainties from the
208 experiments described here, we performed a high number of replications, which allows an
209 average and standard deviation for the SR of each deployment. In the wind experiments, true
210 replication was not possible, as wind speed varied slightly between each deployment. While
211 they cannot be called replicates, we performed a very large number of individual experiments,
212 which allowed for the derivation of a robust relationship between SR and wind speed.
213 Additionally, the variable length of the experiments at selected wind speeds not only added to
214 the number of data points, but also allowed us to assess if there was any effect of deployment
215 time on SR .

216 2.3 Analyses

217 Total Hg (THg) in the activated carbon sorbent was quantified using thermal combustion,
218 amalgamation, and atomic absorption spectroscopy in oxygen (O_2) carrier gas (USEPA Method
219 7473) using an AMA254 (Leco Instruments Ltd.) (USEPA, 2007). Because the sorbent in a PAS
220 cannot be assumed to take up Hg homogeneously, the entire carbon from each PAS was
221 analyzed in two aliquots of up to 0.45 g each. In order to increase the lifetime of AMA254
222 catalyst tubes while processing samples with high sulphur content, catalyst tubes were
223 amended with 5 g of sodium carbonate (Na_2CO_3) and ≈ 0.15 g of Na_2CO_3 was added directly to
224 each sample boat (McLagan et al., 2017). Samples were dried for 30 seconds at 200 °C and

225 thermally decomposed at 750 °C for 330 seconds, while gaseous elemental Hg was trapped on
226 the gold amalgamator. After combustion the system was purged for 60 seconds to ensure all
227 pyrolysis gases were removed from the catalyst. Throughout the analysis the catalyst was
228 heated to 550 °C. After purging, the amalgamator was heated to 900 °C for 12 seconds to
229 release the trapped Hg into the cuvette where absorption at 253.65 nm was measured by dual
230 detector cells for both low and high absolute amounts of Hg.

231 The instrument was calibrated by adding varying amounts of Hg liquid standard for AAS ($1000 \pm$
232 5 mg l^{-1} ; in 10 % w/w HCl; Inorganic Ventures) to $\approx 0.22 \text{ g}$ of clean (unexposed) HGR-AC. $\approx 0.15 \text{ g}$
233 of Na_2CO_3 was added on top of the liquid standard and HGR-AC. In all experiments absolute
234 amounts of Hg were less than 20 ng and the high cell was therefore not required for
235 quantification. The low cell calibration included standards of 0, 0.1, 0.25, 0.5, 1, 2.5, 5, 10, 15,
236 and 20 ng of Hg (uncertainty in autopipette is $1 \pm 0.004 \text{ ng}$) fitted with a quadratic relationship.

237 **2.4 Quality Assurance and Control**

238 Both analytical and field blanks were included in all experiments. Analytical blanks represented
239 analyses of clean HGR-AC with mean concentration of $0.3 \pm 0.2 \text{ ng g}^{-1}$ of HGR-AC (n=14). Field
240 blanks, taken both at the start and end of each experiment, were taken to the site, opened,
241 deployed, and then immediately taken down, sealed with PTFE tape and stored for analysis in
242 double resealable plastic bags. The mean field blank concentration for the wind experiments
243 (n=7), the temperature/RH experiments (n=5), and the Radiello® reuse experiments (n=4) were
244 $0.5 \pm 0.2 \text{ ng g}^{-1}$, $0.58 \pm 0.15 \text{ ng g}^{-1}$ and $0.38 \pm 0.08 \text{ ng g}^{-1}$ of HGR-AC, respectively. All results are
245 blank adjusted by subtracting the mean field blank concentration for each experiment
246 multiplied by the mass of HGR-AC in that sample from the sorbed Hg in each sample.

247 Analytical precision was monitored throughout the experiments (approximately every 10-15
248 instrumental runs) by analyzing 5 or 10 ng Hg liquid Standards for AAS added to $\approx 0.22 \text{ g}$ of HGR-
249 AC. Recoveries for precision testing were 100.1 ± 1.6 (n=62), 100.0 ± 1.3 (n=24), and 100.0 ± 1.3
250 (n=21) % for the wind, temperature/RH, and reuse experiments, respectively. Recovery was
251 monitored throughout the experiments (approximately every 10-15 runs) by analyzing a high

252 sulphur, bituminous coal standard reference material, NIST 2685c (S = 5 wt %; National Institute
253 of Standards and Technology), or our own in-house reference material, RM-HGR-AC1
254 (powdered HGR-AC loaded with Hg by exposure to air for four months then homogenized; 23.1
255 ± 0.8 ng g⁻¹ based on 198 analytical runs). Recoveries of NIST 2685c were 101 ± 3 (n=35), $102 \pm$
256 3 (n=14), and 99 ± 4 (n=10) % for the wind, temperature/RH, and reuse experiments,
257 respectively. Recoveries of RM-HGR-AC1 were 98 ± 3 (n=43), 97 ± 2 (n=13), and 96 ± 2 (n=10) %
258 for the wind, temperature/RH, and reuse experiments, respectively. All statistical tests were
259 either performed by hand or using R v3.3.2 (R Foundation for Statistical Computing).

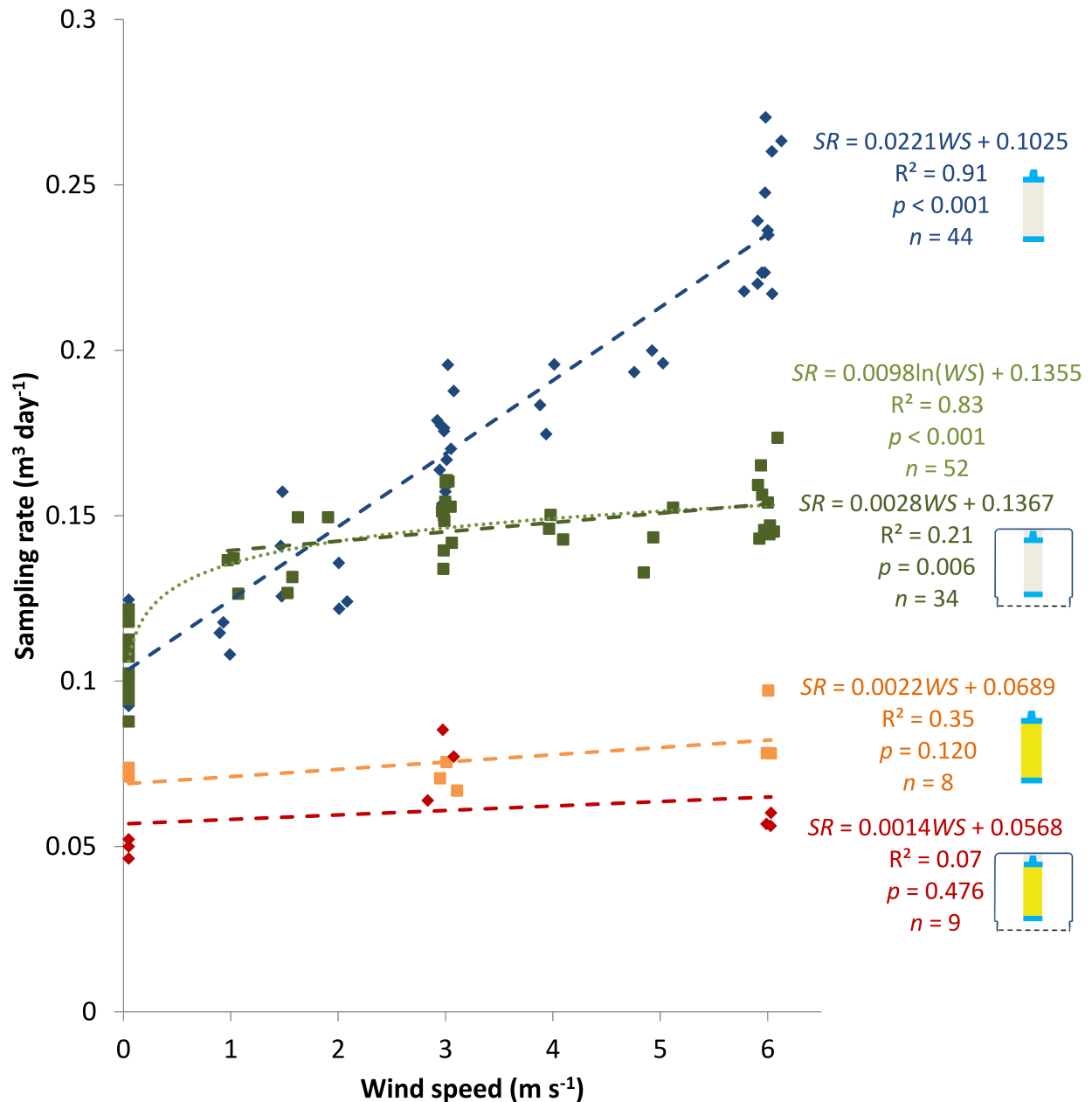
260 3. RESULTS AND DISCUSSION

261 3.1 Wind

262 The effect of wind speed on *SR* varied considerably across the four tested PAS configurations
263 (Fig. 1). The greatest effect was observed for white Radiello® without windshield (configuration
264 2), which is a configuration that is unlikely to be used in practice ($r^2 = 0.91$; $p < 0.001$; $n = 44$).
265 The positive linear relationship across the tested wind speed range (wind still to 6 m s⁻¹) had a
266 slope indicative of a 0.022 m³ day⁻¹ (or 18 % of the calibrated *SR*) increase in *SR* for every 1 m s⁻¹
267 increase in wind speed (Fig. 1). Previous investigators, using the white Radiello® (without
268 protective shield) to monitor varying atmospheric contaminants, fitted logarithmic (Pennequin-
269 Cardinal et al., 2005; Plaisance, 2011; Skov et al., 2007) or quadratic (Plaisance et al., 2004)
270 relationships to data describing the effect of wind speed on *SR*. The *SR* was most sensitive at lower
271 wind speed (typically < 1 m s⁻¹). However, due to the limited number or range of measured wind
272 speeds, or high data uncertainty, a linear relationship fits some of these data equally well
273 (McLagan et al., 2016a).

274 The addition of the windshield (configuration 1), which is the current method of practice,
275 reduced the effect of wind speed on the *SR*, particularly at higher wind speeds. The best fit of
276 the data was a logarithmic relationship (linear fit: $r^2 = 0.83$; $p < 0.001$ for exponentially
277 transformed data; $n = 52$) in which *SR* was most sensitive to wind speed between 0 and 1 m s⁻¹
278 (Fig. 1). While average wind speeds of less than 1 m s⁻¹ are common for indoor deployments,

279 outdoors average wind speeds typically exceed 1 m s^{-1} (98.3 % of data from $0^\circ 10'$ resolution
280 global data set of monthly averaged wind speeds at 10 m above ground level between 1961
281 and 1990 (New et al., 2002)). When we consider only the data $>1 \text{ m s}^{-1}$ we observe a slight, but
282 significant, positive linear relationship between *SR* and wind speed ($r^2 = 0.21$; $p = 0.006$; $n = 34$)
283 corresponding to a $0.003 \text{ m}^3 \text{ day}^{-1}$ (or 2.5 % of the previously calibrated *SR*) increase in *SR* for
284 every m s^{-1} increase in wind speed (Fig. 1). Neither configuration with the thicker, yellow
285 Radiello[®] led to a significant effect ($p > 0.05$) of wind speed on *SR* (Fig. 1). When the protective
286 shield is in place the *SR* was approximately 10 % lower than without the protective shield for
287 the yellow Radiello[®]. Plaisance (2011) also noted a negligible effect of wind speed on *SR* using a
288 yellow Radiello[®] PAS without any protective shield when monitoring benzene.



289

290 **Figure 1: The effect of wind speed on the sampling rate of four different configurations of a passive air**
 291 **sampler for gaseous mercury. Configuration 1: White Radiello®, with protective shield (■);**
 292 **Configuration 2: White Radiello®, without protective shield (); Configuration 3: Yellow Radiello®,**
 293 **with protective shield (■); Configuration 4: White Radiello®, without protective shield (). Standard**
 294 **error of slope and y-intercept are give in Table S1.**

295 The importance of a diffusive barrier is illustrated by the very strong effect of wind speed on
 296 the SR of another PAS for gaseous Hg that also utilizes an activated carbon sorbent, but has no
 297 diffusive barrier: the SR increased by $0.126 \text{ m}^3 \text{ day}^{-1}$ (or 97 % of the calibrated SR) for every m s^{-1}

298 ¹ increase in wind speed (Guo et al., 2014; Zhang et al., 2012). This information and the results
299 here demonstrate the merit of employing both diffusive barriers and protective shield in
300 reducing the effect of wind speed on *SR*. The diffusive path length of the PAS has three
301 components: (1) the ASBL, (2) the diffusive barrier (adjusted for the porosity of the diffusive
302 barrier), and (3) the internal airspace of the Radiello® (McLagan et al., 2016b). Employing a
303 thicker, less porous diffusive barrier (yellow Radiello®) increases the diffusive path length of the
304 diffusive barrier component, in turn reducing the *SR*. By reducing turbulence on the outside of
305 the diffusive barrier, the protective shield essentially increases the thickness of the ASBL
306 (McLagan et al., 2016b), leading to a reduction in *SR*.

307 Because the samplers were not exposed to exactly the same wind speeds, it is not possible to
308 construct uptake curves from the experiments with variable deployment length. It is, however,
309 possible to test whether the measured *SRs* depend on the length of each PAS deployment. The
310 relationship between deployment length and *SR* was not significant ($p > 0.05$), irrespective of
311 the applied wind speed (wind-still, $\sim 3 \text{ m s}^{-1}$, and $\sim 6 \text{ m s}^{-1}$) or configuration (1 and 2); see Fig. S4
312 for details. This confirms that the *SRs* derived from short one-week deployments were neither
313 biased high or low.

314 The 3-month uptake experiment under wind-still conditions produced a *SR* of $0.106 \pm 0.009 \text{ m}^3$
315 day^{-1} when calculated as the average of each PAS deployment (see Fig. S5 for uptake curve).
316 The slope of the regression of m against $C*t$ (McLagan et al., 2016b; Restrepo et al., 2015) gave
317 a very similar *SR* of $0.109 \pm 0.009 \text{ m}^3 \text{ day}^{-1}$. Because the latter method is thought to give a
318 slightly more reliable *SR* (McLagan et al., 2016b; Restrepo et al., 2015), we suggest to use this
319 *SR* for indoor deployments of the PAS using the white Radiello and a windshield (configuration
320 1). This *SR* is 9.9 % lower than the *SR* obtained in an earlier outdoor calibration study, despite
321 the higher temperature ($\sim 23^\circ\text{C}$) indoors than outdoors (mean temperature across all
322 deployments: 7.6°C). Additionally, the replicate precision of samplers from this uptake
323 experiment for the wind-still data with the protective shield ($11 \pm 8 \%$) was significantly poorer
324 ($p < 0.001$) than in the outdoor calibration study with the same sampler setup ($2 \pm 1.3 \%$; mean
325 wind speed 1.89 m s^{-1}) (McLagan et al., 2016b). Both the lower *SR* and the greater uncertainty

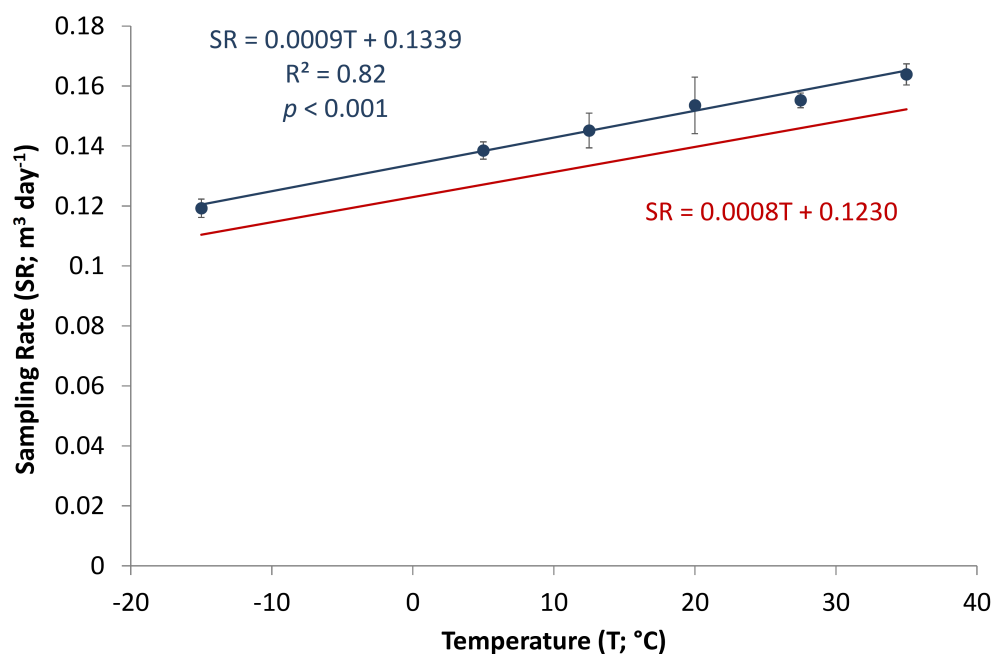
326 of the *SR* are consistent with the effect of wind observed for this configuration (green markers
327 in Fig. 1): At the low wind speeds of indoor deployments ($< 1 \text{ m s}^{-1}$), the *SR* is expected to be
328 both lower and more sensitive to changes in wind speed. Although, conditions for this
329 experiment were labelled “wind-still”, in reality any activity within the laboratory (movement of
330 lab personnel, opening and closing of doors, etc.) will result in small variations in wind speeds
331 around the PAS within the range where the *SR* is most sensitive to such variations (Zhang et al.,
332 2013). Thus, for indoor deployments of the passive sampler, especially using the white
333 Radiello[®], we can expect somewhat less precise results. The effect of laboratory activity may
334 also cause disturbances in the wind measured at higher wind speed treatments. Wind speeds
335 could only be measured for 5 mins before and after each experiment and there may be some
336 difference between measured and actual average wind speed for each deployment. These
337 issues may have contributed to the higher variability in the wind experiments compared to the
338 temperature and relative humidity experiments (see below), which were conducted in closed
339 chamber experiments.

340 **3.2 Temperature and relative humidity**

341 Relative humidity, tested at 44, 60, and 80 % and a stable temperature of 20 °C, had no
342 significant effect on *SR* ($p = 0.080$; see Fig. S6). Relative humidity, tested at 44, 60, and 80 % and
343 a stable temperature of 20 °C, had no significant effect on *SR* ($r^2 = 0.11$; $p = 0.080$; $n = 13$; see
344 Fig. S6), which is similar to Guo et al., (2014) who also observed no effect from relative humidity
345 on the *SR* of their PAS that uses the same sulphur-impregnated activated carbon sorbent. It is
346 therefore appropriate to analyze the effect of temperature on *SR* despite small variations in RH
347 at different temperature levels. We observed a significant, positive, linear relationship between
348 *SR* and temperature ($r^2 = 0.82$; $p < 0.001$; $n = 36$; Fig. 2) corresponding to a $0.001 \text{ m}^3 \text{ day}^{-1}$
349 increase in *SR* for every 1 °C increase in temperature (or 0.7 % of the calibrated *SR*). This
350 relationship remained linear across the tested range from -15 to 35 °C.

351 Temperature can affect the *SR* because of its impact on (i) the partitioning equilibrium between
352 the sorbent and the gas phase and (ii) the diffusion coefficient (McLagan et al., 2016a;
353 Pennequin-Cardinal et al., 2005). The uptake capacity of the HGR-AC for gaseous Hg is

354 extremely high and we suspect that any change in the sorption equilibrium caused by changing
355 temperatures should have a negligible effect on the SR. The increase in diffusivity caused by an
356 increase in temperature is easily quantified. Fig. 2 also displays *SR* as a function of temperatures
357 predicted with a previously described model based on Fick's first law of diffusion (McLagan et
358 al., 2016b). While the predicted *SR*s are ~8 % lower than the measured ones, the slope of the
359 relationship between *SR* and temperature is the same (no significant difference, z-score test, p
360 = 0.427), confirming that the effect of temperature on the diffusivity of gaseous Hg is sufficient
361 to explain the observed temperature dependence of the *SR*.



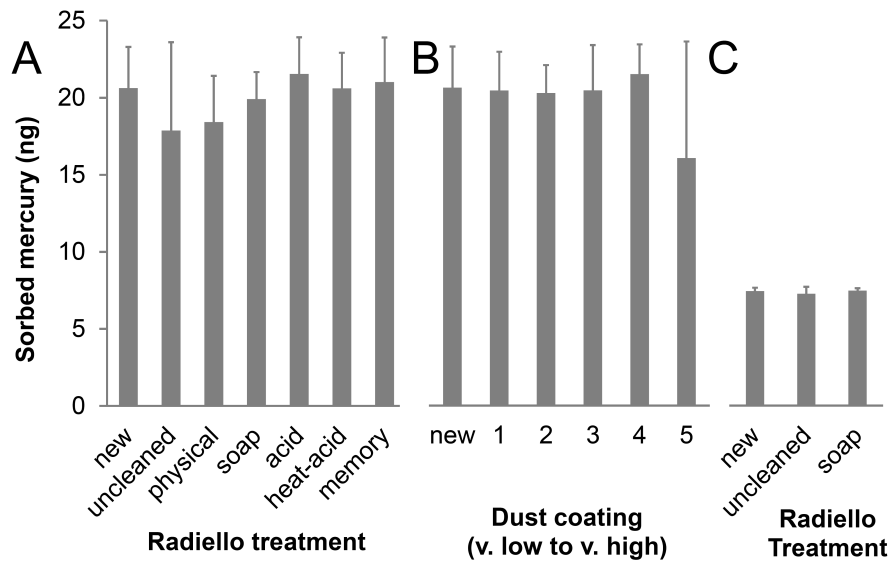
362
363 **Figure 2: The effect of temperature on the sampling rate of a passive air sampler for gaseous mercury**
364 **as determined experimentally (blue) and as calculated using the diffusion model (red) by McLagan et**
365 **al. (2016b). The measured and calculated temperature dependence, given by the slopes of the**
366 **relationships, are not significantly different.**

367 Earlier studies on PAS for gaseous Hg did not observe an effect of temperature on *SR* in
368 laboratory chamber experiments. Guo et al. (2014) found no significant effect of temperature
369 on the *SR* of their activated carbon-based PAS between -10 and +35 °C. Similarly, there was no
370 effect of temperature on the *SR* of a PAS using a solid gold sorbent and a white Radiello®
371 diffusive body (Skov et al., 2007). In neither case, however, was the precision of the
372 measurement sufficient to detect the small dependence of *SR* on temperature caused by the

373 effect of temperature on diffusivity. Such a small temperature effect can only be detected in a
374 highly precise sampler.

375 **3.3 Radiello® reuse**

376 In the Radiello® reuse experiment conducted indoors, no significant difference in the amount of
377 sorbed Hg was observed between *new*, *uncleaned*, or any of the cleaned Radiellos® (ANOVA, p
378 = 0.467; Fig. 3(A)). Similarly, when we ignore the effect of cleaning, no significant difference in
379 the sorbed amount of Hg was observed between Radiellos® with different degrees of dust
380 coatings, including the new Radiellos® (ANOVA, p = 0.841; Fig. 3(B)). The cleaning treatments
381 also did not differ in terms of the observed variances (Levene's Test, p = 0.307). However, the
382 amount of Hg taken up in Radiellos® with the most dust (category 5) had a significantly higher
383 variance than all other treatments (p = 0.004, Levene's Test with Tukey's Honest Significant
384 Difference post hoc test). Although the differences between all Radiello® treatments in the
385 indoor Radiello® reusability experiments are small, the significantly higher variability observed
386 for Radiellos® with the highest dust coating suggests some form of cleaning would be better in
387 maintaining the high level of precision of this PAS. Effect size, using Cohen's d value (see S5),
388 was then applied to examine differences in treatments without the use of traditional binary
389 hypotheses testing (See Table S4). In comparison to new Radiellos® *soap*, *acid*, and *heat-acid*
390 were the most effective treatments. While there was no significant difference in means
391 (ANOVA; p = 0.548) or variances (Levene's; p = 0.221) for the outdoor experiment testing *new*,
392 *uncleaned*, and *soap* Radiellos®, effect size analysis (see S5) confirmed that *soap* cleaning is an
393 effective method in preparing used Radiellos® for redeployment (Fig. 3(C)).



394
 395 **Figure 3: Mean sorbed mercury for differing Radiello® cleaning treatments and at varying degrees of**
 396 **HGR-AC dust coating inside the Radiello® (Panel B) from indoor experiment. Cleaning treatments and**
 397 **degree of dust coating is described in Sect. 2.2.3. Panel A also includes the memory effect treatment,**
 398 **which were uncleaned Radiellos® from deployments in a high concentration environment. Panel C**
 399 **presents the mean sorbed mercury for differing Radiello® cleaning treatments from outdoor**
 400 **experiment.**

401 Uptake of Hg in uncleaned Radiellos® previously deployed in gaseous Hg concentrations 2 – 4
 402 orders of magnitude higher than the other Radiellos® (*memory* treatment) was also not
 403 significantly different from any of the other treatments in terms of mean (ANOVA: $p = 0.499$) or
 404 variance (Levene's: $p = 0.307$; Fig. 3(A)). This implies that very little Hg was sorbed to the
 405 Radiello® and re-released during the subsequent deployment and that gaseous Hg has little
 406 affinity for the porous high-density polyethylene diffusive membrane of the Radiello®.

407 4. RECOMMENDATIONS AND CONCLUSIONS

408 While the *SR* of the PAS in its standard configuration (white Radiello® with protective shield)
 409 was found to depend on both wind speed and temperature, the effects are both small and
 410 predictable. The accuracy of volumetric air concentrations derived from the PAS can be
 411 improved by applying adjustment factors to the *SR*, especially for deployments at or close to
 412 background gaseous Hg concentrations. The *SR* of the standard configuration PAS (white
 413 Radiello® with shield) deployed outdoors of $0.121 \text{ m}^3 \text{ day}^{-1}$ was obtained for a mean wind
 414 speed of 1.89 m s^{-1} and a mean temperature of 7.6°C .¹⁵ We recommend to use the increments

415 from Fig. 1 and Fig. 2, i.e. $0.003 \text{ m}^3 \text{ day}^{-1}$ increase in *SR* for every m s^{-1} increase in wind speed
416 and $0.001 \text{ m}^3 \text{ day}^{-1}$ increase in *SR* for every $1 \text{ }^\circ\text{C}$ increase in temperature to adjust the *SR* of
417 $0.121 \text{ m}^3 \text{ day}^{-1}$ to the average temperature and wind speed of each PAS deployment (See S6 for
418 *SR* adjustment equation and sample calculation).

419 The experiments here predict a *SR* of $0.142 \text{ m}^3 \text{ day}^{-1}$ for an average wind speed of 1.89 m s^{-1}
420 (Fig. 1) and a *SR* of $0.141 \text{ m}^3 \text{ day}^{-1}$ for an average temperature of 7.6°C (Fig. 2). Both these
421 values are greater than the *SR* of $0.121 \text{ m}^3 \text{ day}^{-1}$ from the calibration study (McLagan et al.,
422 2016b). While we presently do not know the reason for this discrepancy, it may be related to
423 the relatively short deployment periods used in the present experiments. As mentioned above,
424 short deployment at background concentrations yield a *SR* with a higher uncertainty. Also,
425 McLagan et al. (2016b) observed that *SR* for PAS deployed outdoors for less than 1-2 months
426 were higher than the *SR* derived for the entire one-year sampling period. Despite this slight
427 discrepancy, we note that the y-intercepts of the relationships reported here (the magnitude of
428 the *SR*) are less important than their slopes (i.e. the temperature and wind speed adjustment
429 factors). An ongoing study measuring the uptake of gaseous Hg in PAS deployed at several
430 locations with widely different temperature and wind speed conditions will help refine both the
431 *SR* applicable to outdoor deployments and the validity of the laboratory derived adjustment
432 factors for temperature and wind speed reported here.

433 When designing a PAS, there is a need to strike a balance between maximizing the *SR* and
434 minimizing the variability in the *SR* caused by factors such as wind speed, objectives that are
435 contradictory in nature (McLagan et al., 2016a). Although using a thicker, yellow Radiello® with
436 or without a protective shield are the methods least affected by wind, the *SR* for these methods
437 is approximately half that of the white Radiello® with a shield. A lower *SR* translates to lower
438 amounts of sorbed Hg, which means that longer deployments are required to reach method
439 quantification limits (MQL). The PAS configuration with white Radiello® and windshield needs
440 to be exposed to typical background concentrations of gaseous Hg ($\sim 1.5 - 2 \text{ ng m}^{-3}$) for
441 approximately one week to reach levels above MQL (McLagan et al., 2016b). A PAS with yellow
442 Radiello would presumably require deployments twice as long. For either configuration, longer

443 deployments of a month or more are likely to yield greater accuracy. Given the possibility of
444 adjusting the *SR* for the slight effect caused by wind speeds above 1 m s^{-1} and the shorter
445 minimum deployment times, we recommend the PAS configuration with a shielded white
446 Radiello for most outdoor deployments. Nonetheless, there may be long deployments under
447 highly variable winds that warrant the use of the yellow Radiello®. A full long-term calibration
448 study outdoors would be advisable prior to using this configuration.

449 Finally, our results suggest that previously deployed Radiello® are indeed reusable as long as
450 the Radiellos® are cleaned between deployments. Because the different cleaning methods were
451 generally equally effective, we recommend the use of the *soap* method because of its overall
452 ease and health, safety and waste benefits over using acids (Anastas and Warner, 1998).
453 Additionally, Gustin et al., (2011) suggested the porosity of high density poly-ethylene diffusive
454 barriers can be affected by cleaning with HCl. While in this study we used HNO₃ for cleaning
455 purposes, the possibility of porosity changes caused by acid cleaning is further incentive to
456 clean previously used Radiellos® with *soap* rather than *acid* or *heat-acid* treatments.

457 **Data Availability**

458 Data can be found in the paper, the SI, or via communication with the corresponding author.

459 **Competing Interests**

460 The authors declare that they have no conflicts of interest.

461 **Acknowledgements**

462 We acknowledge funding from Strategic Project Grant #463265-14 by the Natural Sciences and
463 Engineering Research Council of Canada (NSERC) and an NSERC Alexander Graham Bell Canada
464 Graduate Scholarship. We thank S. Steffen of Environment and Climate Change Canada for the
465 loan of the Tekran instrument and B. Branfireun, S. Bartlett, C. Hamilton, and A. Craig from
466 Western University for providing access to the BIOTRON facility.

467 **References**

468 Anastas, P. T., and Warner, J. C.: Green chemistry: Theory and practice, Oxford University Press,
469 New York, USA, 152 pp., 1998.

470 Armitage, J. M., Hayward, S. J., and Wania, F.: Modeling the uptake of neutral organic chemicals
471 on XAD passive air samplers under variable temperatures, external wind speeds and ambient
472 air concentrations (PAS-SIM), *Enviro. Sci. Technol.*, 47, 13546-13554, 2013.

473 Bartkow, M. E., Booij, K., Kennedy, K. E., Müller, J. F., and Hawker, D. W.: Passive air sampling
474 theory for semivolatile organic compounds, *Chemosphere*, 60, 170-176,
475 <http://dx.doi.org/10.1016/j.chemosphere.2004.12.033>, 2005.

476 Brown, R. J. C., Kumar, Y., Brown, A. S., and Kim, K.-H.: Memory effects on adsorption tubes for
477 mercury vapor measurement in ambient air: elucidation, quantification, and strategies for
478 mitigation of analytical bias, *Environ. Sci. Technol.*, 45, 7812-7818, 2011.

479 Brown, R. J. C., Burdon, M. K., Brown, A. S., and Kim, K.-H.: Assessment of pumped mercury
480 vapour adsorption tubes as passive samplers using a micro-exposure chamber, *J. Environ.
481 Monitor.*, 14, 2456-2463, 10.1039/C2EM30101F, 2012.

482 Cole, A. S., and Steffen, A.: Trends in long-term gaseous mercury observations in the Arctic and
483 effects of temperature and other atmospheric conditions, *Atmos. Chem. Phys.*, 10, 4661-4672,
484 10.5194/acp-10-4661-2010, 2010.

485 Driscoll, C. T., Mason, R. P., Chan, H. M., Jacob, D. J., and Pirrone, N.: Mercury as a global
486 pollutant: sources, pathways, and effects, *Environ. Sci. Technol.*, 47, 4967-4983, 2013.

487 Guo, H., Lin, H., Zhang, W., Deng, C., Wang, H., Zhang, Q., Shen, Y., and Wang, X.: Influence of
488 meteorological factors on the atmospheric mercury measurement by a novel passive sampler,
489 *Atmos. Environ.*, 97, 310-315, 2014.

490 Gustin, M. S., Lyman, S. N., Kilner, P., and Prestbo, E.: Development of a passive sampler for
491 gaseous mercury, *Atmos. Environ.*, 45, 5805-5812,
492 <http://dx.doi.org/10.1016/j.atmosenv.2011.07.014>, 2011.

493 Huang, J., Lyman, S. N., Hartman, J. S., and Gustin, M. S.: A review of passive sampling systems
494 for ambient air mercury measurements, *Environ. Sci. Process. Impacts*, 16, 374-392, 2014.

495 Lozano, A., Usero, J., Vanderlinden, E., Raez, J., Contreras, J., and Navarrete, B.: Air quality
496 monitoring network design to control nitrogen dioxide and ozone, applied in Malaga, Spain,
497 *Microchem. J.*, 93, 164-172, <http://dx.doi.org/10.1016/j.microc.2009.06.005>, 2009.

498 McLagan, D. S., Mazur, M. E. E., Mitchell, C. P. J., and Wania, F.: Passive air sampling of gaseous
499 elemental mercury: a critical review, *Atmos. Chem. Phys.*, 16, 3061-3076, 10.5194/acp-16-3061-
500 2016, 2016a.

501 McLagan, D. S., Mitchell, C. P. J., Huang, H., Lei, Y. D., Cole, A. S., Steffen, A., Hung, H., and
502 Wania, F.: A High-Precision Passive Air Sampler for Gaseous Mercury, *Environ. Sci. Technol.*
503 *Lett.*, 3, 24-29, 10.1021/acs.estlett.5b00319, 2016b.

504 McLagan, D. S., Huang, H., Lei, Y. D., Wania, F., and Mitchell, C. P. J.: Prevention of catalyst
505 poisoning in automated atomic absorption spectroscopy instruments for analysis of total
506 mercury samples with high sulphur content, *Spectrochim. Acta B*, 133, 60-62, 2017.

507 Moeckel, C., Harner, T., Nizzetto, L., Strandberg, B., Lindroth, A., and Jones, K. C.: Use of
508 deuration compounds in passive air samplers: Results from active sampling-supported field
509 deployment, potential uses, and recommendations, *Environ. Sci. Technol.*, 43, 3227-3232, 2009.

510 New, M., Lister, D., Hulme, M., and Makin, I.: A high-resolution data set of surface climate over
511 global land areas, *Climate research*, 21, 1-25. URL of data:
512 <https://crudata.uea.ac.uk/cru/data/hrg/tmc/>, 2002.

513 Pennequin-Cardinal, A., Plaisance, H., Locoge, N., Ramalho, O., Kirchner, S., and Galloo, J.-C.:
514 Performances of the Radiello® diffusive sampler for BTEX measurements: Influence of
515 environmental conditions and determination of modelled sampling rates, *Atmos. Environ.*, 39,
516 2535-2544, <http://dx.doi.org/10.1016/j.atmosenv.2004.12.035>, 2005.

517 Peterson, C., Gustin, M., and Lyman, S.: Atmospheric mercury concentrations and speciation
518 measured from 2004 to 2007 in Reno, Nevada, USA, *Atmos. Environ.*, 43, 4646-4654,
519 <http://dx.doi.org/10.1016/j.atmosenv.2009.04.053>, 2009.

520 Pirrone, N., Cinnirella, S., Feng, X., Finkelman, R., Friedli, H., Leaner, J., Mason, R., Mukherjee,
521 A., Stracher, G., and Streets, D.: Global mercury emissions to the atmosphere from
522 anthropogenic and natural sources, *Atmos. Chem. Phys.*, 10, 5951-5964, 2010.

523 Plaisance, H., Sagnier, I., Saison, J., Galloo, J., and Guillermo, R.: Performances and application
524 of a passive sampling method for the simultaneous determination of nitrogen dioxide and
525 sulfur dioxide in ambient air, *Environ. Monitor. Assess.*, 79, 301-315, 2002.

526 Plaisance, H., Piechocki-Minguy, A., Garcia-Fouque, S., and Galloo, J. C.: Influence of
527 meteorological factors on the NO₂ measurements by passive diffusion tube, *Atmos. Environ.*,
528 38, 573-580, <http://dx.doi.org/10.1016/j.atmosenv.2003.09.073>, 2004.

529 Plaisance, H.: The effect of the wind velocity on the uptake rates of various diffusive samplers,
530 *International Journal of Environmental Analytical Chemistry*, 91, 1341-1352,
531 [10.1080/03067311003782625](http://dx.doi.org/10.1080/03067311003782625), 2011.

532 Restrepo, A. R., Hayward, S. J., Armitage, J. M., and Wania, F.: Evaluating the PAS-SIM model
533 using a passive air sampler calibration study for pesticides, *Environ. Sci. Process. Impacts*, 17,
534 1228-1237, 2015.

535 Rutter, A. P., Snyder, D. C., Stone, E. A., Schauer, J. J., Gonzalez-Abraham, R., Molina, L. T.,
536 Márquez, C., Cárdenas, B., and de Foy, B.: In situ measurements of speciated atmospheric
537 mercury and the identification of source regions in the Mexico City Metropolitan Area, *Atmos.*
538 *Chem. Phys.*, 9, 207-220, [10.5194/acp-9-207-2009](http://dx.doi.org/10.5194/acp-9-207-2009), 2009.

539 Selin, N. E.: Global biogeochemical cycling of mercury: a review, *Annu. Rev. Env. Resour.*, 34, 43-
540 63, [doi:10.1146/annurev.enviro.051308.084314](http://dx.doi.org/10.1146/annurev.enviro.051308.084314), 2009.

541 Shoeib, M., and Harner, T.: Characterization and comparison of three passive air samplers for
542 persistent organic pollutants, *Environ. Sci. Technol.*, 36, 4142-4151, 2002.

543 Skov, H., Sørensen, B. T., Landis, M. S., Johnson, M. S., Sacco, P., Goodsite, M. E., Lohse, C., and
544 Christiansen, K. S.: Performance of a new diffusive sampler for Hg⁰ determination in the
545 troposphere, *Environ. Chem.*, 4, 75-80, <http://dx.doi.org/10.1071/EN06082>, 2007.

546 Steffen, A., Douglas, T., Amyot, M., Ariya, P., Aspö, K., Berg, T., Bottenheim, J., Brooks, S.,
547 Cobbett, F., Dastoor, A., Dommergue, A., Ebinghaus, R., Ferrari, C., Gardfeldt, K., Goodsite, M.
548 E., Lean, D., Poulain, A. J., Scherz, C., Skov, H., Sommar, J., and Temme, C.: A synthesis of
549 atmospheric mercury depletion event chemistry in the atmosphere and snow, *Atmos. Chem.*
550 *Phys.*, 8, 1445-1482, 10.5194/acp-8-1445-2008, 2008.

551 Steffen, A., Scherz, T., Olson, M., Gay, D., and Blanchard, P.: A comparison of data quality
552 control protocols for atmospheric mercury speciation measurements, *J. Environ. Monitor.*, 14,
553 752-765, 2012.

554 UNEP: Minamata Convention on Mercury: Text and Annexes, United Nations Environmental
555 Programme, Geneva, Switzerland, 67, 2013.

556 USEPA: Method 7473: Mercury in solids and solutions by thermal decomposition,
557 amalgamation, and atomic absorption spectrophotometry, United States Environmental
558 Protection Agency, Washington, 17, 2007.

559 Zhang, W., Tong, Y., Hu, D., Ou, L., and Wang, X.: Characterization of atmospheric mercury
560 concentrations along an urban–rural gradient using a newly developed passive sampler, *Atmos.*
561 *Environ.*, 47, 26-32, <http://dx.doi.org/10.1016/j.atmosenv.2011.11.046>, 2012.

562 Zhang, X., Brown, T. N., Ansari, A., Yeun, B., Kitaoka, K., Kondo, A., Lei, Y. D., and Wania, F.:
563 Effect of wind on the chemical uptake kinetics of a passive air sampler, *Environ. Sci. Technol.*,
564 47, 7868-7875, 2013.